Physics Letters A 381 (2017) 1831–1836

Contents lists available at ScienceDirect

Physics Letters A

www.elsevier.com/locate/pla

Aharonov–Bohm effect in bilayer graphene

Chang-Soo Park

Department of Physics, Dankook University, Cheonan 330-714, Republic of Korea

ARTICLE INFO

Article history:
Received 30 November 2016
Received in revised form 24 March 2017
Accepted 24 March 2017
Available online 29 March 2017
Communicated by L. Ghivelder

Keywords:
Aharonov–Bohm effect
Trigonal warping
Bilayer graphene

ABSTRACT

We investigate Aharonov–Bohm effect in bilayer graphene. We consider a setup of n–$p(n')$–n junction with Aharonov–Bohm loop connected in the transmission region. In the presence of trigonal warping we show that, due to the anisotropic dispersion of eigenspectrum, the Aharonov–Bohm interference depends on the geometry of junction: it exists for armchair interface but vanishes for zigzag interface. For the armchair interface, it is demonstrated that the period of Aharonov–Bohm oscillation is $\Phi_0 = h/e$ and the amplitude of oscillation can be varied with incident energy and the barrier height of the junction.

1. Introduction

The Aharonov–Bohm (AB) effect [1], a pure quantum phenomenon based on quantum interference, has been studied in many areas of physics. Experimentally, the effect was proved by measuring phase shift due to the AB interference [2–4]. In solid-state material the AB effect was observed in mesoscopic metal ring [5] and carbon nanotubes [6,7]. In recent years, the study of AB effect in monolayer graphene (MLG) has also attracted much interest because of its peculiar electronic transport property stemming from the linear dispersion of energy spectrum and extra degrees of freedom such as sublattice and valley [8]. Several experimental observations of the AB effect in MLG with ring geometry, including some special features not observed in metal and semiconductor, have been reported [9–11]. The AB effect in a MLG ring, in conjunction with confinement potential, has also been exploited to produce valley polarized persistent currents [12].

While there have been extensive studies on the AB effect with MLG no investigation of the effect has been performed for a bilayer graphene (BLG) which has more diverse electronic properties [13]. In this paper, we investigate the AB effect in BLG. In particular, we are interested in the influence of trigonal warping (TW) on the AB effect. In BLG with Bernal stacking, due to the direct interlayer hopping between $A1$ and $B2$ sites, a trigonal warping is introduced in the energy spectrum. This term breaks the rotational symmetry of the 2D energy dispersion, which yields anisotropic transport of quasiparticles. As we shall show below when these quasiparticles pass through a n–$p(n')$–n junction initially valley-degenerate waves emerge as valley-dependent waves in the transmission region. We examine the interference of these waves after traveling an AB loop via separate path.

We demonstrate that the AB interference is sensitive to the orientation of BLG at the interface of the junction. For armchair interface the isoenergy contour is symmetric about the normal direction of incidence, whereas it becomes asymmetric for zigzag interface. From these properties, it is found that the AB interference survives for armchair interface but it disappears for zigzag interface. For the armchair interface, numerical simulations show that the AB conductance oscillates with period $\Phi_0 (= h/e)$ and the oscillation amplitude can be varied with the barrier height of the junction as well as the incident energy.

2. Aharonov–Bohm conductance

In this section we describe our model and derive a formula for the AB conductance of the model. We will consider two cases, armchair interface and zigzag interface.

2.1. Armchair interface

Consider a BLG n–$p(n')$–n junction with armchair interfaces where the $p(n')$ region is a rectangular barrier with width d and height V_0 and the right n region includes a hexagonal AB loop through which a magnetic flux Φ is threaded (see Fig. 1). In the presence of TW the low-energy effective Hamiltonian of BLG is expressed as [13]

$$\hat{\mathcal{H}}_\tau = \left(\frac{-p_x^2 + p_y^2}{2m} + \tau v_3 p_x \right) \hat{\sigma}_x - \left(\tau \frac{p_x p_y}{m} + v_3 p_y \right) \hat{\sigma}_y , \qquad (1)$$

E-mail address: olnal@dankook.ac.kr.

http://dx.doi.org/10.1016/j.physleta.2017.03.043
0375-9601/

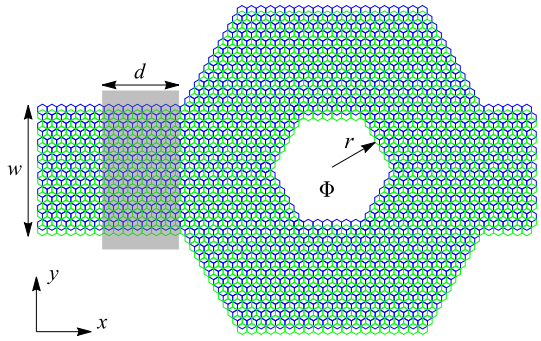

Fig. 1. Bilayer graphene n–$p(n')$–n junction with armchair interfaces and hexagonal Aharonov–Bohm loop. The gray region indicates potential barrier ($p(n')$ region). Φ is the magnetic flux threading the hole of the loop.

where $\hat{\sigma}_{x,y}$ are the Pauli matrices, $p_{x,y} = -i\hbar\partial_{x,y}$, $m = \gamma_1/2v_F^2 \simeq 0.043m_e$ is an effective mass ($\gamma_1 \simeq 0.4$ eV), $v_3 = \gamma_3 v_F/\gamma_0 \simeq 0.12v_F$ is the TW term ($\gamma_3 \simeq 0.38$ eV, $\gamma_0 \simeq 3.16$ eV, $v_F \simeq 10^6$ m/s), and τ is the valley index with $\tau = +1$ for K valley and $\tau = -1$ for K' valley. In the area of AB loop with magnetic flux we use the substitution $p_{x,y} \to \Pi_{x,y} = p_{x,y} + eA_{x,y}$ and choose Landau gauge for the vector potential such that $\mathbf{A} = (0, Bx, 0)$ which preserves the translational invariance along the y direction. The uniform perpendicular magnetic field B is threaded the inner hole of the loop to produce magnetic flux $\Phi = 2\sqrt{3}Br^2$. In the following we will assume $L_{x,y} \lesssim l_B$, where $L_{x,y}$ are the linear sizes of AB loop and $l_B = \sqrt{\hbar/eB}$ is a magnetic length. It will also be assumed that the two arms of AB loop are symmetric about the normal direction of incidence (the x-axis) and their widths as well as those of the left and right leads are large enough that the edge effects due to boundary conditions can be neglected [14,15].

In the incidence and transmission regions the eigenspectrum and pseudospinor of the Hamiltonian (1) are given by

$$
\begin{aligned}
|\chi_\tau\rangle &= \frac{1}{\sqrt{2}}\begin{pmatrix} 1 \\ -e^{i\tau\delta_\tau} \end{pmatrix}, \\
\delta_\tau &= \arctan\frac{\epsilon_k \sin 2\phi + \tau\epsilon_3 \sin\phi}{\epsilon_k \cos 2\phi - \tau\epsilon_3 \cos\phi}, \\
E_\tau(k,\phi) &= \sqrt{\epsilon_k^2 + \epsilon_3^2 - 2\tau\epsilon_k\epsilon_3 \cos 3\phi}\,,
\end{aligned}
\tag{2}
$$

where $\epsilon_k = \hbar^2k^2/2m$, $\epsilon_3 = \hbar k v_3$ and $\phi = \arctan(k_y/k_x)$ with $\mathbf{k} = (k_x, k_y)$ being the wave vector. The TW term ϵ_3 distorts isoenergy curves for the eigenspectrum $E_\tau(\mathbf{k})$ to have anisotropic dispersion. As a result, for a given wave vector $\mathbf{k}$, the group velocity $\mathbf{v}_\tau = (1/\hbar)\nabla_k E_\tau(\mathbf{k})$ of one valley is different from the other. Because of this valley-dependent transport property initially valley-degenerate incident waves, after transmitting the barrier, will appear as valley-dependent waves with different transmission amplitudes T_K and $T_{K'}$.

In Fig. 2 we plot some examples of transmission probabilities as a function of incident angle and barrier height for the armchair interface. It can be seen that the transmissions from each valley are different in the anisotropic dispersion (second and third rows) while there is no valley-dependent transmission in the isotropic dispersion (first row). We note that, for the armchair interface, the angle-dependent transmissions are distributed symmetric about the normal incidence, which can be expected from the isoenergy curve (see Fig. 3 below).

Taking into account the valley-dependent transmitted waves, the total wave in the interference region can be expressed as

$$
|\psi\rangle = \sum_{\tau=\pm}\sum_{s=\pm} T_\tau(\phi_s)|\chi_\tau(\phi_s)\rangle|\mathbf{k}_\tau(\phi_s)\rangle\, e^{i\alpha_s}\,, \tag{3}
$$

where $\tau = \pm$ represent the valleys as before and the index s depicts the spatial dependence of polarized waves through the incident angle ϕ_s such that

$$
-\frac{\pi}{2} \le \phi_- \le 0\,, \quad 0 \le \phi_+ \le \frac{\pi}{2}\,. \tag{4}
$$

Thus, ϕ_+ (ϕ_-) is associated with waves propagating upper (lower) arm of the AB loop and $\alpha_\pm$ are the corresponding AB phases given by

$$
\alpha_\pm = \frac{2\pi}{\Phi_0}\int_{\pm}^{} \boldsymbol{A}\cdot d\boldsymbol{r} \quad \left(\Phi_0 = \frac{h}{e}\right). \tag{5}
$$

The momentum states $|\mathbf{k}_\tau(\phi_s)\rangle$ denote plane waves, satisfying orthogonality condition

$$
\begin{aligned}
&\langle\mathbf{k}_{\tau'}(\phi_{s'})|\mathbf{k}_\tau(\phi_s)\rangle = \delta_{\tau'\tau}\,\delta\left(\mathbf{k}_{\tau'}(\phi_{s'}) - \mathbf{k}_\tau(\phi_s)\right), \\
&\mathbf{k}_\tau(\phi_s) = k_\tau(\phi_s)\left(\mathrm{sgn}(s)\cos\phi_s\,\mathbf{e}_x - \mathrm{sgn}(s)\sin|\phi_s|\,\mathbf{e}_y\right).
\end{aligned}
\tag{6}
$$

Here, the valley and angle-dependent magnitude $k_\tau(\phi)$ is determined by equating an incident energy ϵ with the eigenspectrum $E_\tau(\mathbf{k})$ in (2). For a given incident energy ϵ, the orthogonal condition $\delta_{\tau'\tau}$ disallows interference between inter-valley waves. The remaining condition then requires $k_\tau(\phi_{s'}) = k_\tau(\phi_s)$ and $\phi_{s'} = \pm\phi_s$, which, for the interference between the waves from upper and lower arms, leads to $k_\tau(\phi_-) = k_\tau(\phi_+)$ with $\phi_- = -\phi_+$. For armchair interface this condition is satisfied because the isoenergy contour of the eigenspectrum (2) is symmetric about $\phi = 0$ as illustrated in Fig. 3: this is also seen from the symmetric transmissions of each valley in Fig. 2. In terms of transmission amplitude, the only surviving interference terms are $T_\tau^*(\phi_+)T_\tau(\phi_-)$ and its complex conjugate.

To investigate the AB effect in the present model we consider conductance across the sample. We start with an angle-dependent (and also valley-dependent) velocity in the interference region, defined as

$$
\mathbf{v}_\tau(\phi) = \langle\psi|\hat{\mathbf{v}}_\tau|\psi\rangle\,, \quad \hat{\mathbf{v}}_\tau = \frac{1}{i\hbar}\left[\hat{\mathbf{r}},\ \hat{\mathcal{H}}_\tau\right], \tag{7}
$$

where the explicit forms of velocity operator $\hat{\mathbf{v}}_\tau$ and velocity $\mathbf{v}_\tau(\phi)$ are, respectively, given in Eqs. (A.1) and (A.2). Unlike isotropic transmission the velocity $\mathbf{v}_\tau(\phi)$ cannot be decoupled from the transmission amplitudes due to the angle-dependent magnitude $k_\tau(\phi)$. To proceed we take an average of the velocity over incident angle ϕ, defined as

$$
\langle\mathbf{v}_\tau\rangle = \frac{1}{2\phi_{\tau c}}\int_{-\phi_{\tau c}}^{\phi_{\tau c}} \mathbf{v}_\tau(\phi)\,d\phi\,. \tag{8}
$$

Here, due to the anisotropic property of isoenergy contour, the range of incident angles depends on valley and given by $|\phi| \le \phi_{\tau c}$, where the limit $\phi_{\tau c}$ is determined by the condition $\mathbf{v}_{\tau x}^{in} = (1/\hbar)\left[\nabla_k E_\tau(\mathbf{k})\right]_x \ge 0$. Using (2) this condition reads

$$
\frac{\hbar}{m}k_\tau(\phi)\cos(\delta_\tau(\phi) - \phi) - \tau v_3\cos\delta_\tau(\phi) \ge 0\,. \tag{9}
$$

Employing the properties $\delta_\tau(-\phi) = -\delta_\tau(\phi)$ and $k_\tau(-\phi) = k_\tau(\phi)$ and using the expression of $\mathbf{v}_\tau(\phi)$ in Eq. (A.2), the angle average will cancel the y component and we obtain

$$
\langle\mathbf{v}_\tau\rangle = \frac{\hbar}{2m\lambda}\,\frac{1}{2\phi_{\tau c}}\int_{-\phi_{\tau c}}^{\phi_{\tau c}} \sigma_\tau(\alpha,\phi)d\phi\,, \tag{10}
$$